Synthesis of hydrolytically and oxidation-responsive networks using thiol-ene "click" chemistry with pentaerythritol tetrakis(3-mercaptopropionate) and tri/tetra-acrylates

Article

Accepted Version

Kazybayeva, D. S., Irmukhametova, G. S. and Khutoryanskiy, V. (2021) Synthesis of hydrolytically and oxidation-responsive networks using thiol-ene "click" chemistry with pentaerythritol tetrakis(3-mercaptopropionate) and tri/tetra-acrylates. Polymers for Advanced Technologies, 32 (7). pp. 2682-2689. ISSN 1042-7147 doi: https://doi.org/10.1002/pat.5147 Available at https://centaur.reading.ac.uk/93710/

Synthesis of hydrolytically and oxidation responsive networks using thiol-ene "click" chemistry with pentaerythritol tetrakis(3-mercaptopropionate) and tri/tetra-acrylates

Diara S. Kazybayeva[1], Galiya S. Irmukhametova[1], Vitaliy V. Khutoryanskiy[1,2]*

[1] Al-Farabi Kazakh National University, 71 al-Farabi Av., 050040, Almaty, Kazakhstan

[2] Reading School of Pharmacy, University of Reading, Whiteknights, PO Box 224, RG66AD, Reading, United Kingdom, v.khutoryanskiy@reading.ac.uk

ABSTRACT

Thiol-ene click reactions of pentaerythritol tetrakis(3-mercaptopropionate) with pentaerythritol tetraacrylate and trimethylolpropane triacrylate were used to prepare polymeric degradable networks. The structure and properties of these networks were studied using Fourier-transform infrared and Raman spectroscopy, thermal gravimetric analysis and scanning electron microscopy. Degradation of these materials was evaluated in different media including phosphate buffer with and without esterase as well as in oxidative environment with hydrogen peroxide. Exposure of the samples to these media results in their degradation. Slow hydrolytic degradation was observed in phosphate buffer and it was not accelerated by the presence of an enzyme. Faster degradation is observed in solutions of hydrogen peroxide. The mechanisms of this degradation are discussed.

KEYWORDS: thiol-ene click; networks; biodegradation; thiols; oxidation; hydrolysis

Short running title: Hydrolytically and oxidation responsive networks

This paper is dedicated to 70th anniversary of Prof Sarkyt Kudaibergenov

1. INTRODUCTION

Very efficient chemical reactions of thiol groups with unsaturated molecules containing either double or triple bonds are known since the early 1900s [1]. However, the last few decades have witnessed the substantially renewed interest in these reactions, which now fall into the category of so-called “click” processes, resulting in the products with high yields, excellent selectivity of bonding, complete absence or ease of byproducts removal, mild conditions to achieve formation of covalent bonds and many other advantages [2].

Thiol-ene click reactions have now become increasingly important in the synthesis of novel polymeric materials [3,4] and also as a tool to conjugate polymers or various labels with biomacromolecules [5,6] or colloids [7–9]. These could proceed through two potential mechanisms, such us thiol-ene radical or thiol Michael-type addition reactions [2].

Polymeric materials capable of degrading in a biological environment (biodegradation) have received interest for different medical applications [10]. They could be used as biodegradable sutures following surgery [11] or as implants capable of releasing active ingredients slowly for a long period of time [12]. Biodegradation of polymers is often related to hydrolytic reactions or oxidation-reduction processes in response to various biological molecules present in the human body. Hydrolytically cleavable synthetic polymers are more commonly used and well researched. These include polyesters such as poly(lactic-co-glycolic acid) copolymers and polycaprolactone) [13,14]. Polymers that undergo degradation in response to oxidative conditions (e.g. reactive oxygen species) are less established and are represented mainly by various polysulfides [15–19]. Potentially, the oxidation-responsive materials could be used for targeting inflammatory reactions.

Previously**,** we have reported the synthesis of nanoparticles through thiol-ene click reaction between pentaerythritol tetrakis(3-mercaptopropionate) (PEMP) and pentaerythritol tetraacrylate (PETA) [20]. Depending on the molar PEMP/PETA ratio these nanoparticles could be formed either with thiol or acrylate groups on the surface. It was demonstrated that thiolated nanoparticles

exhibited mucoadhesive properties, i.e. the ability to stick to mucosal membranes. This property could be useful for applications in certain areas of drug delivery.

Taking into consideration that the networks formed as a result of thiol-ene click reactions between PEMP and PETA will have potentially hydrolytically cleavable ester bonds and oxidation-responsive thioether bonds it was hypothesized that these materials may exhibit biodegradable properties. The present work reports the synthesis of polymeric networks through the thiol-ene reactions of pentaerythritol tetrakis(3-mercaptopropionate) with tri- and tetra-acrylates, their physicochemical characterisation and studies of biodegradability in various media *in vitro*.

2. MATERIALS AND METHODS

2.1. Materials

N,N-dimethylformamide (DMF), pentaerythritol tetraacrylate (PETA), trimethylolpropane triacrylate (TMPTA), pentaerythritol tetrakis(3-mercaptopropionate) (PEMP), and porcine liver esterase (PLE) were purchased from Sigma-Aldrich (UK). All other chemicals were of analytical grade and used without further purification.

2.2. Synthesis

Polymer samples of different ratios and concentrations of initial monomer mixture were synthesized in the presence of N,N-dimethylformamide (DMF) as described in [20]. DMF used in this synthesis was used as received without any degassing with inert gas. Initial monomer mixture was based on pentaerythritol tetraacrylate (PETA) or trimethylolpropane triacrylate (TMPTA) as "ene" compounds and pentaerythritol tetrakis(3-mercaptopropionate) (PEMP) as thiol-containing compound. Synthesis was performed at 30°C up to one hour with constant stirring which resulted in transparent slightly rubbery gels. Synthesized gels were washed in DMF for one hour and then three times in acetone to remove unreacted monomers. After this procedure they were exposed to water for some time to wash acetone out and freeze-dried for further characterisation. Each

synthesis was repeated independently at least 3 times and the resulting networks exhibited reproducible properties.

2.3. Swelling ability

The swelling ability of cross-linked polymers was estimated by measuring the weight of the dry samples submerged in different solvents at room temperature. The weighed samples were placed in vials containing the solvent and stored at room temperature for several days. Solvents that were used are water, ethanol and chloroform. The samples were weighed every 2 days after removing excess of solvents from their surfaces. The degrees of swelling (DS) were calculated according to the following equation:

$$DS = (m_{swollen} - m_{dry})/m_{dry}$$

where $m_{swollen}$ and m_{dry} are the weights of swollen and dry samples, respectively.

The mean values were calculated based on the analysis of samples in triplicates.

2.4. FTIR- and Raman spectroscopy

FTIR analysis was performed on PE Spectrum 100 FTIR spectrometer (Perkin-Elmer, USA) for the range of 650-4200 cm^{-1}. Nicolet NXR 9650 FT Raman spectrometer (Thermo Scientific, UK) was used to record Raman spectra of the samples.

2.5. Thermogravimetric analysis

Thermal gravimetric analysis of the samples was performed using Q50 TGA analyser (TA Instruments, UK). The polymer samples were heated from 25 to 600 °C at a heating rate of 10 °C min^{-1} and a flow of nitrogen at 50 $mL \cdot min^{-1}$. Samples were approximately 5 mg each.

2.6. Scanning electron microscopy

Morphology and structure of the samples were characterized using SEM with FEI Quanta 600 FEG Environmental Scanning Electron Microscope instrument (FEI UK Ltd., UK) at an acceleration voltage of 20 kV. The images were taken from both the surface and the fractured part of the samples. Prior to SEM experiments the samples were sputter-coated with gold. Pore size of samples was measured by analysing SEM images using ImageJ 1.52a software.

2.7. Biodegradation studies

Biodegradation ability was studied in different media such as phosphate buffered saline (pH=7.4) with and without addition of esterase and solutions of hydrogen peroxide of different concentrations. Dry samples of known mass were immersed in 10 mL of different degradation media for several weeks with a continuous shaking at 37°C. Samples were weighted every day after carefully wiping out excess of moisture with a tissue paper.

2.8. Preparation of the media for biodegradation studies

Phosphate buffer saline was prepared by dissolving 21.8 g Na_2HPO_4, 6.4 g NaH_2PO_4, 180 g NaCl in 1 L of deionized water. Before use it was diluted 1:20 with deionized water and pH was adjusted if necessary.

Hydrogen peroxide solutions of different concentrations were prepared by dilution of its 30 % solution with deionized water. The exact concentrations of these solutions were determined using permanganate titration. Hydrogen peroxide solution of unknown concentration in a 25 mL volumetric flask was adjusted to the mark with water and mixed thoroughly. An aliquot of the analyzed solution with a volume of 2 mL was pipetted into a flask for titration, 2 mL of 1 mol/L sulfuric acid solution was added, and titrated with a solution of 0.05 mol/L potassium permanganate until a stable pink color appeared. Titration was carried out at least 5 times until reproducible results were recorded.

The mass of hydrogen peroxide $m_i(H_2O_2)$ in the analysed solution for each titration was calculated according to the formula for direct titration of the analyte:

$$m_i(H_2O_2) = \frac{c(^1/_5\, KMnO_4) \cdot V_i(KMnO_4)}{V_a(H_2O_2)} \cdot M(^1/_2\, H_2O_2) \cdot V_f(H_2O_2)$$

where $c(^1/_5\, KMnO_4)$ is the molar equivalent concentration of potassium permanganate; $V_i(KMnO_4)$ is the volume of potassium permanganate used for titration; $V_a(H_2O_2)$ is the aliquot

volume of analysed solution; $M(^1/_2 H_2O_2)$ is the molar mass of equivalent and $V_f(H_2O_2)$ is the volumetric flask volume.

The molar mass of the hydrogen peroxide equivalent is determined based on the half-reaction:

$$H_2O_2 \leftrightarrow 2H^+ + O_2 + 2e$$

Mass fraction of hydrogen peroxide was calculated as follows:

$$w(H_2O_2) = \frac{m_i}{m_{weight}} \cdot 100\%$$

where m_i is the mass of hydrogen peroxide and m_{weight} is the mass of initial sample.

3. RESULTS AND DISCUSSION

3.1. Synthesis

Thiol-ene click reaction of PEMP with pentaerythritol tetraacrylate (PETA) and trimethylolpropane triacrylate (TMPTA) was simply promoted through the use of dimethylformamide as a solvent, similarly to our previous report [20].

Figure 1 shows the reaction scheme describing the formation of a crosslinked network based on PETA-PEMP combination. New covalent thioether bonds were formed as a result of this reaction. Similar reaction was also observed in the case of TMPTA-PEMP. The resulting products were formed as slightly rubbery transparent materials.

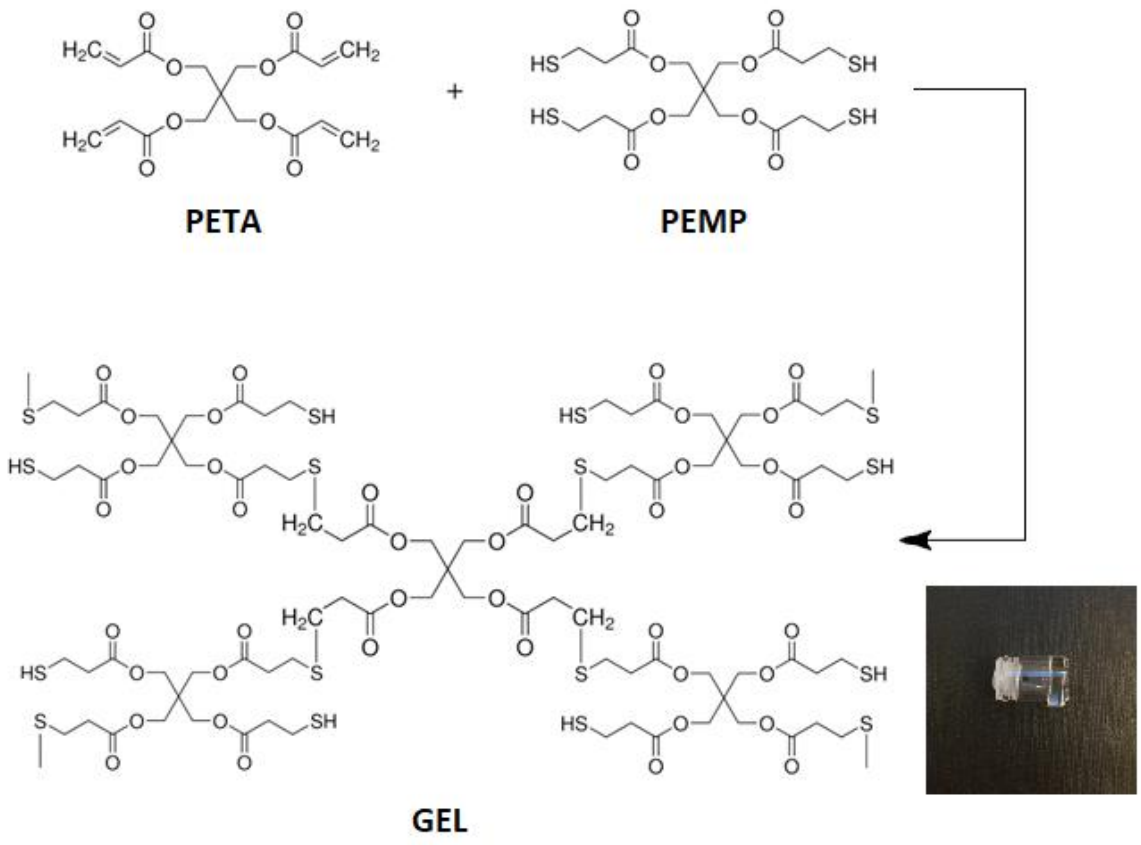

Figure 1. Proposed scheme describing the reaction between PETA and PEMP resulting in formation of a cross-linked network. Insert: an exemplary image of a cross-linked network as a result of this reaction.

It should be noted that formation of a transparent gel was only observed when the reagents were used in equimolar (1:1 mol/mol) ratios or when the excess of PETA or TMPTA was used to PEMP (3:1 mol/mol).The mixtures of PETA or TMPTA with PEMP containing the excess of PEMP (1:3) did not form gels. This is consistent with our previous publication [20] reporting that formation of gels is observed only at specific component ratios and monomer concentrations in dimethylformamide.

When these gel samples were immersed in the excess of water they lost their transparency and turned white. This change of transparency is possibly related to the hydrophobic nature of

these networks, which can swell well in dimethylformamide but contract when this solvent is replaced with water.

3.2. Swelling of networks in water, ethanol and chloroform

The ability of the samples to swell in water, ethanol and chloroform was evaluated by their immersion in excess of these solvents for several days. After reaching the swelling equilibrium within 4 days in a solvent the samples were withdrawn, weighed, dried and re-weighed again to calculate the degrees of swelling. The swelling results for samples immersed in water and ethanol are summarized in Table 1. It was not possible to evaluate the degrees of swelling of the network samples in chloroform because upon immersion in this solvent all gels disintegrated into small pieces within couple of hours.

Table 1

The network samples immersed in water and ethanol retained their shapes and exhibited very poor ability to swell. For example, a sample prepared from PETA-PEMP (1:1) absorbed only up to 0.013±0.005 g of water per 1 g of dry polymer. Similar levels of swelling were observed for all samples both in water and ethanol; however, the swelling in ethanol was slightly higher in some cases. This indicates that the nature of these materials is hydrophobic similarly to PLGA [13]. The hydrophobic nature of these materials is also confirmed by swelling and subsequent disintegration of these gels in chloroform. The hydrophobic nature of these materials and their poor swelling in water are desirable attributes for application as body implants as excessive swelling in bodily fluids could result in unwanted pressure on internal organs.

3.3. Spectral and thermal characterization of dry samples

FTIR spectra for PETA–PEMP and TMPTA-PEMP samples showed a strong band at 1721-1726 cm^{-1} due to C=O stretching vibrations ($\nu_{C=O}$) (Figure 2). FTIR spectra of monomers used for the synthesis of these samples are included in Figures S1-S3 (Supporting information). Samples of 1:1 mol/mol ratio also showed a band at 1286 cm^{-1} due to C-H bend (methylene $–CH_2–$ twisting and wagging), which is not pronounced well for samples with prevailing acrylic content. The band at 1634 cm^{-1} for samples prepared with 3:1 mol/mol ratio indicates the presence of unreacted C=C double bond conjugated with C=O. In the samples with 1:1 mol/mol ratio the band at 1634 cm^{-1} is not present confirming that all C=C bonds reacted with thiol groups of PEMP.

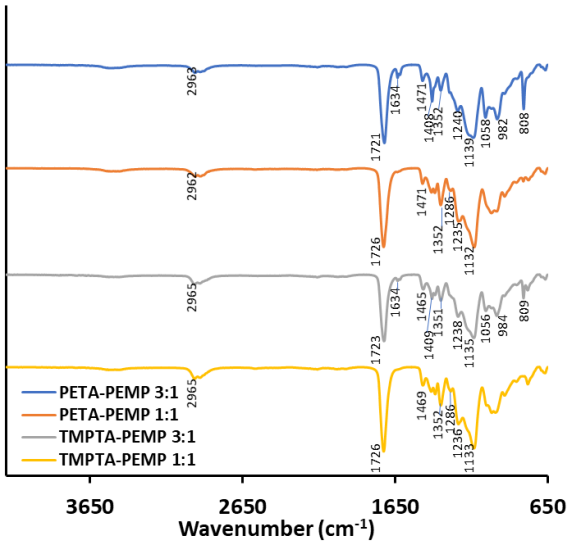

(a)

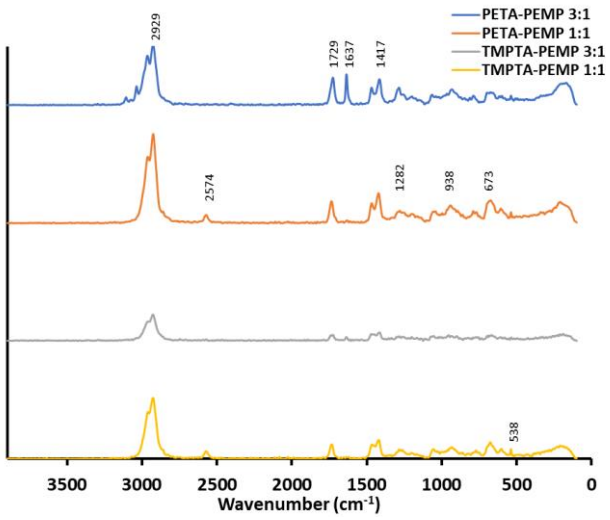

(b)

Figure 2. FTIR (a) and Raman (b) spectra of all synthesised PETA-PEMP and TMPTA-PEMP networks

In order to confirm the presence of thiol groups Raman-spectroscopy was used, since SH-groups have a very distinct band typical for these groups. Raman spectra recorded for PETA–PEMP and TMPTA-PEMP samples, prepared with 1:1 mol/mol ratio, showed strong bands at 2574 cm^{-1} due to S–H stretching (ν_{SH}), 673 cm^{-1} due to ν_{C-S} and 538 cm^{-1} due to ν_{S-S}. Raman spectra of PETA–PEMP and TMPTA-PEMP gels prepared with excess of PETA did not show any bands typical for SH groups, but the strong band responsible for C=C stretching was found at 1637 cm^{-1}. All samples of PETA–PEMP and TMPTA-PEMP gels showed the bands at 2929 cm^{-1} due to C–H stretching (ν_{CH}), 1729 cm^{-1} due to $\nu_{C=O}$, 1417 cm^{-1} and 1282 cm^{-1} due to ν_{CH2}, 938 cm^{-1} due to ν_{C-O-C}, which is consistent with the results of FTIR spectroscopy and also confirms successful click reactions leading to the formation of polymeric structures proposed in Figure 1.

The physical properties of materials designed for biomedical applications should be extensively characterized to evaluate their suitably. One of these important properties is the thermal stability, which may provide useful information about the possibility of sterilization using autoclaving. TGA was used to evaluate the thermal stability of the networks (Figure 3). Both PETA–PEMP and TMPTA-PEMP samples show excellent thermal stability, with decomposition observed only above 345-360 ^{o}C reaching 94-95% of the total weight loss at 500 °C. The thermal

degradation profiles of all four samples are very similar. Samples with excess of PETA or TMPTA (3:1 mol/mol) show slightly higher thermal stability.

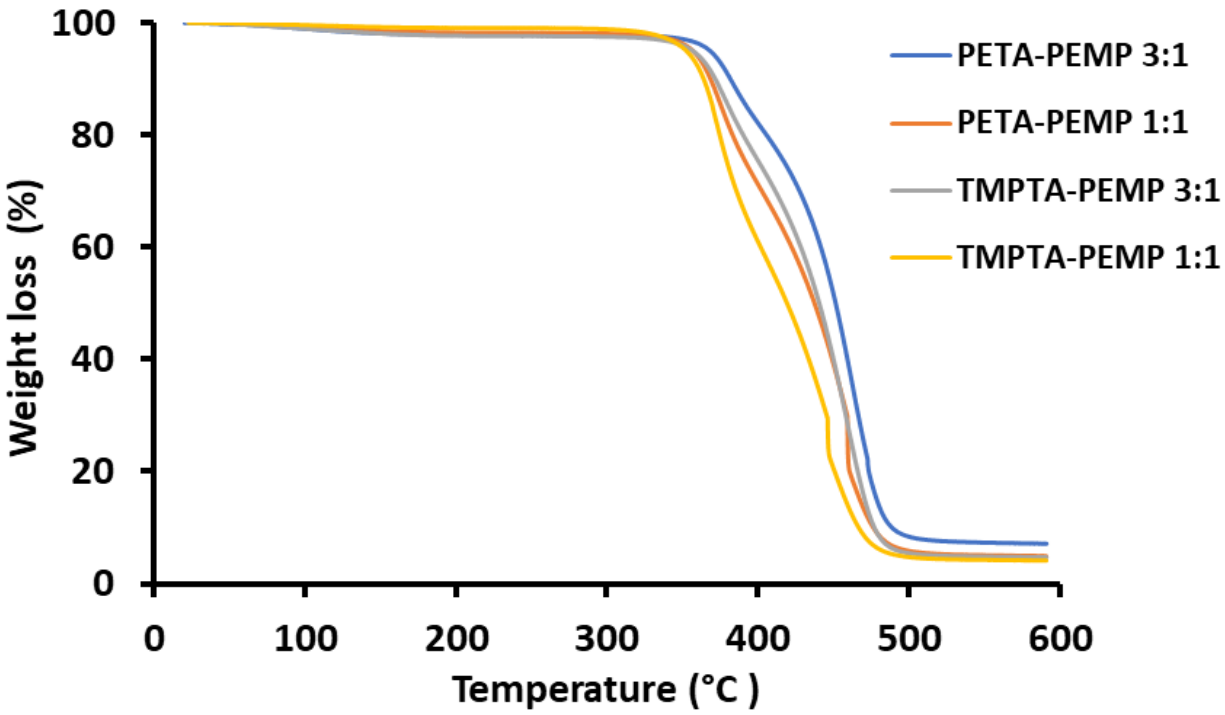

Figure 3. Thermal gravimetric analysis of all the synthesized PETA-PEMP and TMPTA-PEMP dry network samples

3.4. Scanning electron microscopy

The morphology of the polymer gel cross-sections and surfaces were studied using scanning electron microscopy (SEM) (Figure 4). Comparison of PETA-PEMP 1:1 and TMPTA-PEMP 1:1 samples at high magnification (2000×) showed that PETA-containing gels do not have any significant features on both their surface and cross-sections. On the contrary, the TMPTA-PEMP sample cross-sections reveal that the TMPTA-PEMP (3:1 mol/mol) material is porous compared to TMPTA-PEMP (1:1 mol/mol), which is also reflected in the swelling results. The size of pores on the surface of TMPTA-PEMP (3:1 mol/mol) is around 2 μm.

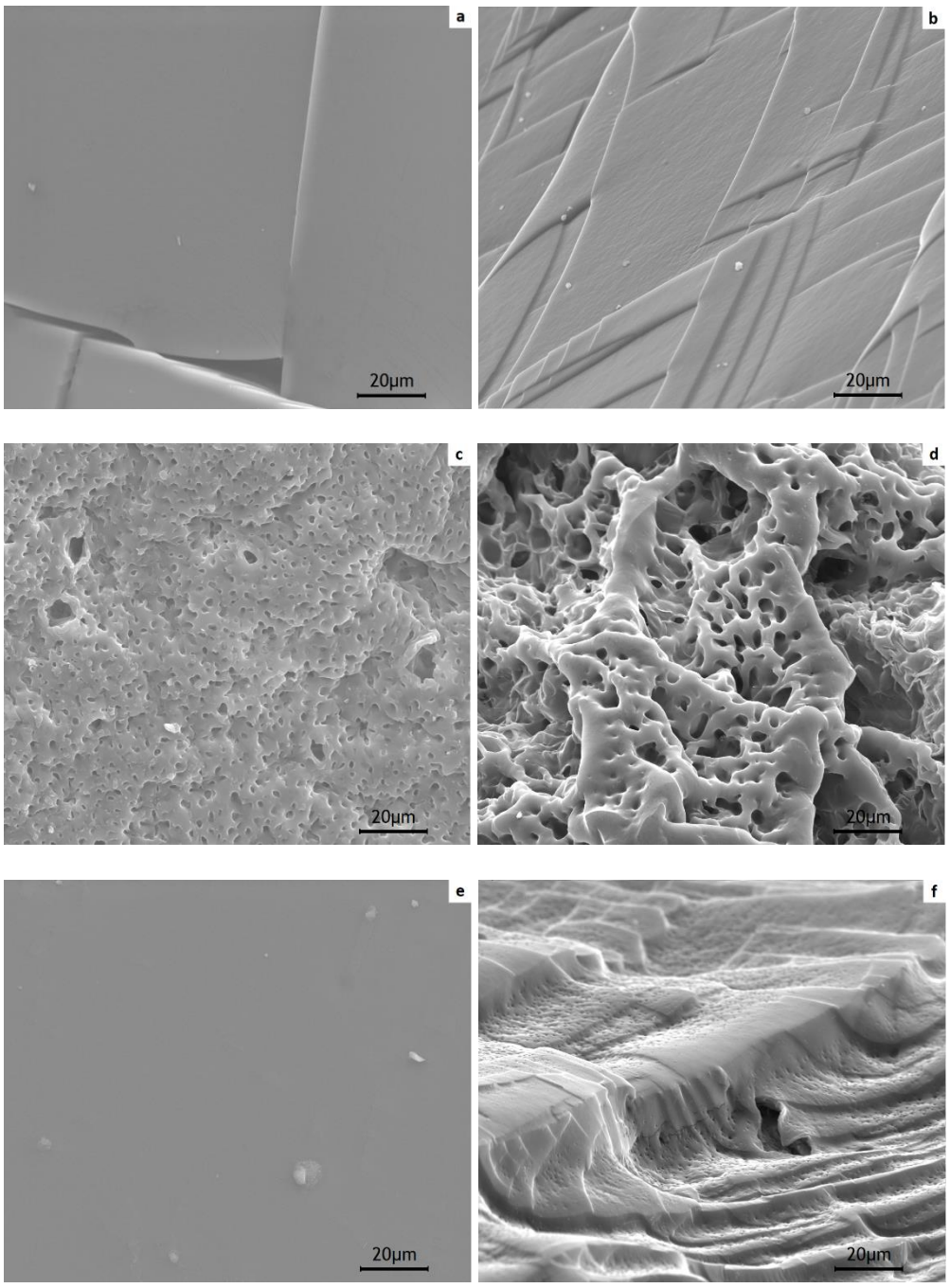

Figure 4. SEM images of PETA-PEMP (1:1 mol/mol) surface (a) and cross-section (b); TMPTA-PEMP (3:1 mol/mol) surface (c) and cross-section (d); TMPTA-PEMP (1:1 mol/mol) surface (e) and cross-section (f).

3.5. Biodegradation studies

Taking the structure of the networks into consideration and the nature of chemical bonds present within these materials it can be hypothesized that they may undergo biodegradation through several pathways. First, the presence of ester bonds may imply that these materials may degrade hydrolytically and this may or may not be facilitated by the presence of an enzyme (e.g. esterase). Second, the presence of $–CH_2$-S-CH_2- bonds indicates the possibility for oxidation-induced degradation, which could convert these hydrophobic groups into more hydrophilic sulfoxides and sulfones. Third, our spectral data indicates the presence of disulfide bridges (-S-S-) in the samples, which resulted from oxidation of thiol groups present in PEMP. These groups may also undergo degradation in the presence of reducing agents.

The degradation of the networks in aqueous media was evaluated gravimetrically. When samples are losing weight it means that they undergo degradation and disintegrate or dissolve. An increase in the sample weight may indicate that the sample becomes more hydrophilic and undergoes swelling. Figure 5 shows the degradation profiles of the samples in phosphate buffer saline with and without esterase as well as in solutions containing hydrogen peroxide. In PBS all samples show an initial degradation with approximately 3-5 % weight loss in the first 7 days. Then the degradation slows down and the sample weight either remains constant or even shows some increase. The increase in the sample weight for TMPTA-PEMP 3:1 PLE could be related to their partial swelling due to more porous structure confirmed by SEM and as a result of the degradation of some bonds and appearance of more hydrophilic regions due to the presence of carboxylic groups. It was surprising to see that the degradation of the samples in the presence of esterase proceeds slower than in the absence of the enzyme. This could be related to the densely cross-linked and hydrophobic nature of the network and inability of enzyme molecules to approach ester bonds and cleave them efficiently. Additionally hydrophobic nature of the samples may cause deposition of enzyme molecules on their surface and their partial immobilization and inactivation. Overall, hydrolytic degradation of hydrophobic polyesters is a very slow process that may take

several months. For example, the mass loss of materials based on poly(D,L-lactide-co-glycolide) caused by hydrolysis in aqueous media also proceeds very slowly within several weeks and months [21, 22].

(a)

(b)

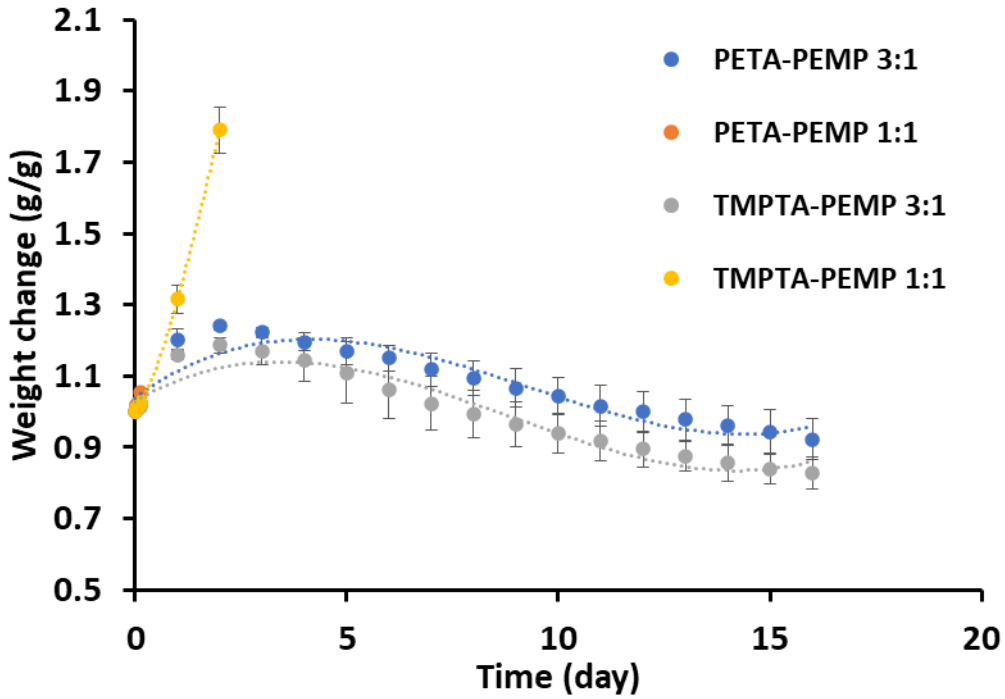

Figure 5. Biodegradation studies showing the changes in sample weights in phosphate buffered saline (pH=7.4) with and without enzyme (a) and in 1.825% H_2O_2 solutions (b). All biodegradation experiments were conducted at 37 °C under continuous shaking. Note that PETA-PEMP 1:1 sample did disintegrate in the first minutes of experiment.

It is known [23] that inflammation in the human body is accompanied by the release of reactive oxygen species such as hydrogen peroxide. This prevents the spread of infection and serves as a signal for attracting white blood cells. The degradation of our samples in the presence of hydrogen peroxide proceeds more intensively compared to hydrolytic degradation. Initially the

samples show swelling and in some compositions, e.g. TMPTA-PEMP 1:1, this is quite substantial. Then after initial swelling both 1:1 samples undergo rapid disintegration into smaller irregularly-shaped pieces and colloidal particles, for which it is not possible to continue gravimetric measurements. Both 3:1 samples show more gradual degradation profiles: after initial swelling within the first three days they begin to reduce their weight. It is clear that the samples with 1:1 ratio there is a larger proportion of HS- and $–CH_2–S-CH_2-$, which undergo oxidation, which eventually leads to their disintegration. The samples with 3:1 ratio have excess of acrylate groups in their structure and fewer bonds that are prone to oxidative cleavage, which results in their more gradual degradation.

In order to get further insights into the mechanisms of degradation the surfaces of some selected samples (TMPTA-PEMP 3:1) exposed to degradative environment were examined using scanning electron microscopy (Figure 6).

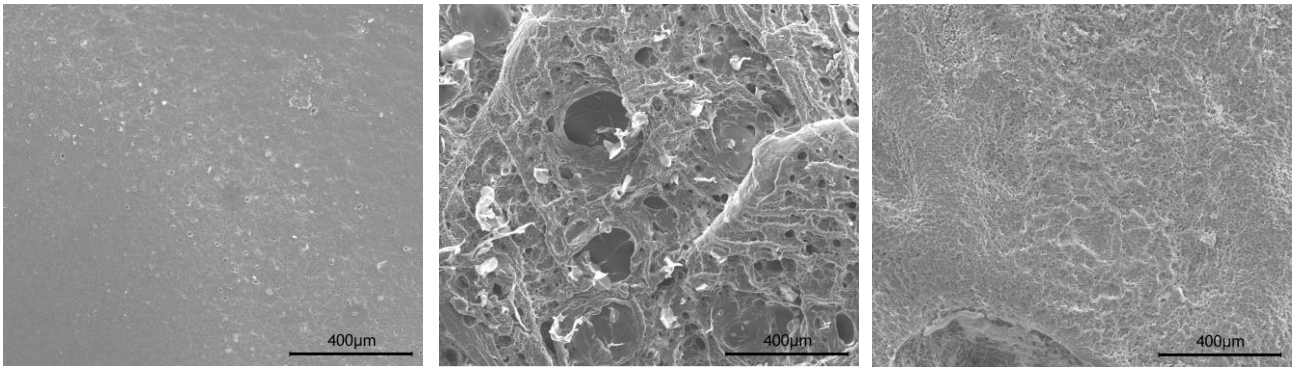

(a) (b) (c)

Figure 6. Scanning electronic microscopy of TMPTA-PEMP 3:1 sample with surfaces: before degradation (a), after biodegradation for 16 days in 1.825% H_2O_2 (b); and after biodegradation for 17 days in PBS with PLE (c). All biodegradation experiments were conducted at 37 °C under continuous shaking.

It is clearly seen that the surface of samples before any degradation is practically non-porous. The degradation in solutions of H_2O_2 leads to formation of a polydisperse system of pores with the presence of both small (22±7 μm) and larger populations (153±71 μm). This is consistent with the gravimetric measurements, which showed that during the degradation process the samples undergo initial swelling. This clearly makes its surface more hydrophilic, rough and porous. Subsequent reduction in the sample weight indicates its gradual degradation and disintegration into smaller pieces. This is also confirmed visually and especially this disintegration becomes more obvious for 1:1 samples. The surface of the sample that was degraded in PBS containing esterase also shows some changes and presence of newly formed small pores of around 8±2 μm. This explains why the hydrolytic degradation of these samples is much less pronounced compared to oxidative process. Formation of small pores does not allow penetration of enzyme molecules into the bulk of the sample, which makes this degradation very slow and not efficient. Additionally esterase may deposit on the surface of the samples and obstruct further penetration.

The mechanism of oxidative degradation of these networks was additionally studied using FTIR spectroscopy (Figure 7). The exposure of samples to hydrogen peroxide solutions leads to clear spectral changes and appearance of several new bands. One of these new bands observed at 1047-1050 cm^{-1} is responsible for sulfoxide groups (-SO-); it does overlap with -C-O- stretch bands (1047-1050 cm^{-1}), but the spectra clearly show the shifts in this area. Another very pronounced new band appeared at 1116 cm^{-1}; this could either be associated with S=O stretch or potentially could be even related to H-O-S bend [24]. These spectral data clearly indicate that the

mechanism of oxidative degradation of these networks is related to oxidation of sulfide bonds with formation of sulfoxide, sulfone and even sulfonate groups (Figure 8).

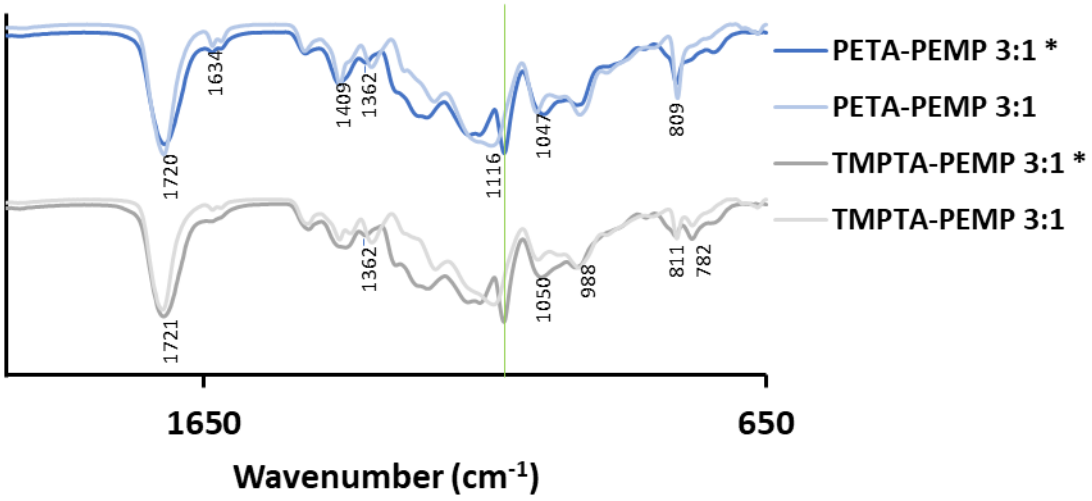

Figure 7. FTIR spectra of PETA-PEMP and TMPTA-PEMP samples before and after biodegradation* in 1.825% H_2O_2 solution at 37°C.

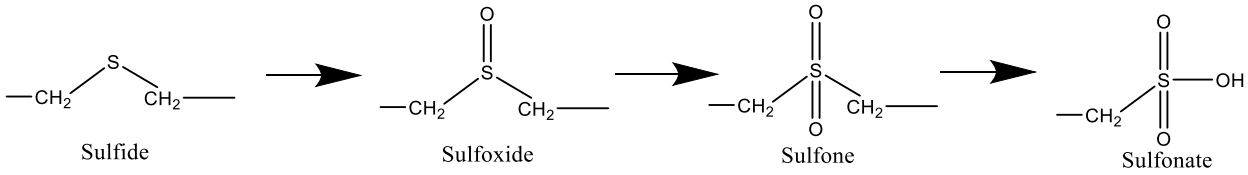

Figure 8. Chemical transformations of sulphide bonds in the networks upon oxidation in hydrogen peroxide

4. Conclusions

Hydrolytically and oxidation responsive networks were prepared from pentaerythritol tetrakis(3-mercaptopropionate) and tri/tetra-acrylates using thiol-ene “click” chemistry. The structure and properties of these materials were characterized using FTIR and Raman spectroscopy, thermal gravimetric analysis and scanning electron microscopy. Biodegradation of these materials was studied under different conditions in vitro. It was established that these networks undergo very

slow hydrolytic degradation and this process is not accelerated in the presence of esterase. Oxidative degradation of these networks proceeds more intensively and in some cases results in a complete disintegration of networks into small particles. These networks could find potential applications as biodegradable implants. Future studies in this case should include evaluation of their biocompatibility *in vitro* and experiments on implantation and biodegradation *in vivo*.

5. References

[1] T. Posner, Beiträge zur Kenntniss der ungesättigten Verbindungen. II. Ueber die Addition von Mercaptanen an ungesättigte Kohlenwasserstoffe, Berichte Der Dtsch. Chem. Gesellschaft. 38 (1905) 646–657. https://doi.org/10.1002/cber.190503801106.

[2] C.E. Hoyle, C.N. Bowman, Thiol–Ene Click Chemistry, Angew. Chemie Int. Ed. 49 (2010) 1540–1573. https://doi.org/10.1002/anie.200903924.

[3] A.B. Lowe, Thiol-ene "click" reactions and recent applications in polymer and materials synthesis, Polym. Chem. 1 (2010) 17–36. https://doi.org/10.1039/B9PY00216B.

[4] A.B. Lowe, Thiol–ene "click" reactions and recent applications in polymer and materials synthesis: a first update, Polym. Chem. 5 (2014) 4820–4870. https://doi.org/10.1039/C4PY00339J.

[5] J.C. Grim, T.E. Brown, B.A. Aguado, D.A. Chapnick, A.L. Viert, X. Liu, K.S. Anseth, A Reversible and Repeatable Thiol–Ene Bioconjugation for Dynamic Patterning of Signaling Proteins in Hydrogels, ACS Cent. Sci. 4 (2018) 909–916. https://doi.org/10.1021/acscentsci.8b00325.

[6] Q.-F. Li, Y. Yang, A. Maleckis, G. Otting, X.-C. Su, Thiol–ene reaction: a versatile tool in site-specific labelling of proteins with chemically inert tags for paramagnetic NMR, Chem. Commun. 48 (2012) 2704–2706. https://doi.org/10.1039/C2CC17900H.

[7] H. Huang, M. Liu, X. Tuo, J. Chen, L. Mao, Y. Wen, J. Tian, N. Zhou, X. Zhang, Y. Wei, One-step fabrication of PEGylated fluorescent nanodiamonds through the thiol-ene click

reaction and their potential for biological imaging, Appl. Surf. Sci. 439 (2018) 1143–1151. https://doi.org/https://doi.org/10.1016/j.apsusc.2017.12.233.

[8] E.D.H. Mansfield, V.R. de la Rosa, R.M. Kowalczyk, I. Grillo, R. Hoogenboom, K. Sillence, P. Hole, A.C. Williams, V. V Khutoryanskiy, Side chain variations radically alter the diffusion of poly(2-alkyl-2-oxazoline) functionalised nanoparticles through a mucosal barrier, Biomater. Sci. 4 (2016) 1318–1327. https://doi.org/10.1039/C6BM00375C.

[9] Y. Liu, W. Hou, H. Sun, C. Cui, L. Zhang, Y. Jiang, Y. Wu, Y. Wang, J. Li, B.S. Sumerlin, Q. Liu, W. Tan, Thiol-ene click chemistry: a biocompatible way for orthogonal bioconjugation of colloidal nanoparticles, Chem. Sci. 8 (2017) 6182–6187. https://doi.org/10.1039/c7sc01447c.

[10] W. Amass, A. Amass, B. Tighe, A review of biodegradable polymers: uses, current developments in the synthesis and characterization of biodegradable polyesters, blends of biodegradable polymers and recent advances in biodegradation studies, Polym. Int. 47 (1998) 89–144. https://doi.org/10.1002/(SICI)1097-0126(1998100)47:2<89::AID-PI86>3.0.CO;2-F.

[11] S. Vainionpää, P. Rokkanen, P. Törmälä, Surgical applications of biodegradable polymers in human tissues, Prog. Polym. Sci. 14 (1989) 679–716. https://doi.org/https://doi.org/10.1016/0079-6700(89)90013-0.

[12] O.S. Manoukian, M.R. Arul, N. Sardashti, T. Stedman, R. James, S. Rudraiah, S.G. Kumbar, Biodegradable polymeric injectable implants for long-term delivery of contraceptive drugs, J. Appl. Polym. Sci. 135 (2018) 46068. https://doi.org/10.1002/app.46068.

[13] H.K. Makadia, S.J. Siegel, Poly Lactic-co-Glycolic Acid (PLGA) as Biodegradable Controlled Drug Delivery Carrier, Polymers (Basel). 3 (2011) 1377–1397. https://doi.org/10.3390/polym3031377.

[14] D. Mondal, M. Griffith, S.S. Venkatraman, Polycaprolactone-based biomaterials for tissue engineering and drug delivery: Current scenario and challenges, Int. J. Polym. Mater. Polym. Biomater. 65 (2016) 255–265. https://doi.org/10.1080/00914037.2015.1103241.

[15] F. El-Mohtadi, R. d'Arcy, N. Tirelli, Oxidation-Responsive Materials: Biological Rationale, State of the Art, Multiple Responsiveness, and Open Issues, Macromol. Rapid Commun. 40 (2019) 1800699. https://doi.org/10.1002/marc.201800699.

[16] E. Lallana, N. Tirelli, Oxidation-Responsive Polymers: Which Groups to Use, How to Make Them, What to Expect From Them (Biomedical Applications), Macromol. Chem. Phys. 214 (2013) 143–158. https://doi.org/10.1002/macp.201200502.

[17] P. Carampin, E. Lallana, J. Laliturai, S.C. Carroccio, C. Puglisi, N. Tirelli, Oxidant-Dependent REDOX Responsiveness of Polysulfides, Macromol. Chem. Phys. 213 (2012) 2052–2061. https://doi.org/10.1002/macp.201200264.

[18] C.D. Vo, G. Kilcher, N. Tirelli, Polymers and Sulfur: what are Organic Polysulfides Good For Preparative Strategies and Biological Applications, Macromol. Rapid Commun. 30 (2009) 299–315. https://doi.org/10.1002/marc.200800740.

[19] V.V. Khutoryanskiy, N. Tirelli, Oxidation-responsiveness of nanomaterials for targeting inflammatory reactions , Pure Appl. Chem. . 80 (2008) 1703. https://doi.org/10.1351/pac200880081703.

[20] A. Štorha, E.A. Mun, V. V. Khutoryanskiy, Synthesis of thiolated and acrylated nanoparticles using thiol-ene click chemistry: towards novel mucoadhesive materials for drug delivery, RSC Adv. 3 (2013) 12275. https://doi.org/10.1039/C3RA42093K.

[21] Boimvaser S., Mariano R.N., Turino L.N., Vega J.R. In vitro bulk/surface erosion pattern of PLGA implant in physiological conditions: a study based on auxiliary microsphere systems, Polym. Bull. 73, 209-227 (2016) https://doi.org/10.1007/s00289-015-1481-6

[22] Farahani T.D., Entezami A.A., Mobedi H., Abtahi M. Degradation of Poly(D,L-lactide-co-

glycolide)50:50 Implant in Aqueous Medium, Iranian Polym. J. 14(8), 753-763 (2005)

[23] C. Wittmann, P. Chockley, S.K. Singh, L. Pase, G.J. Lieschke, C. Grabher, Hydrogen Peroxide in Inflammation : Messenger, Guide, and Assassin, 2012 (2012). https://doi.org/10.1155/2012/541471.

[24] C. Arsene, I. Barnes, K.H. Becker, W.F. Schneider, T.T. Wallington, N. Mihalopoulos, I. V. Patroescu-Klotz, Formation of methane sulfinic acid in the gas-phase OH-radical initiated oxidation of dimethyl sulfoxide, Environ. Sci. Technol. 36 (2002) 5155–5163. https://doi.org/10.1021/es020035u.

Table 1. Degrees of swelling (DS) of samples in water and ethanol

Composition with molar ratios	DS in water	DS in ethanol
PETA-PEMP (3:1)	0.020 ± 0.005	0.070 ± 0.005
PETA-PEMP (1:1)	0.031 ± 0.005	0.032 ± 0.013
TMPTA-PEMP (3:1)	0.065 ± 0.023	0.087 ± 0.026
TMPTA-PEMP (1:1)	0.016 ± 0.011	0.041 ± 0.010